Fractional Quantum-Hall Liquid Spontaneously Generated by Strongly Correlated t_{2g} Electrons

Jörn W. F. Venderbos, Stefanos Kourtis, Jeroen van den Brink, and Maria Daghofer

Institute for Theoretical Solid State Physics, IFW Dresden, 01171 Dresden, Germany

For topologically nontrivial and very narrow bands, Coulomb repulsion between electrons has been predicted to give rise to a spontaneous fractional quantum-Hall (FQH) state in the absence of magnetic fields. Here we show that strongly correlated electrons in a t_{2g}-orbital system on a triangular lattice self-organize into a spin-chiral magnetic ordering pattern that induces precisely the required topologically nontrivial and flat bands. This behavior is very robust and does not rely on fine-tuning. In order to go beyond mean field and to study the impact of longer-range interactions, we map the low-energy electronic states onto an effective one-band model. Exact diagonalization is then used to establish signatures of a spontaneous FQH state.

The integer quantum-Hall (IQH) effect [1] is a prime example of an electronic state that cannot be classified within the traditional framework of symmetry breaking, but is instead characterized by a topological invariant [2]. It is by now theoretically well established that an external magnetic field is in principle not needed and that states within the same topological class as IQH states can be realized in lattice models, if time-reversal symmetry is broken by other mechanisms, e.g., by complex electron hoppings [3]. Related topologically nontrivial quantum spin-Hall (QSH) states even occur in systems where time-reversal symmetry is not broken at all [4–8], see Refs. [9,10] for reviews. At present, many intriguing features intrinsic to topologically nontrivial states have been observed in the absence of magnetic fields, such as the metallic Dirac cones at the surface of a topological insulator [11,12], or the QSH effect in quantum wells [13,14].

Fractional quantum-Hall (FQH) states [15] are topological states that can be seen as composed of quasiparticles carrying an exact fraction of the elementary electronic charge [16]. Apart from the fundamental interest in observing a quasiparticle that behaves in many ways like a fraction of an electron, some FQH states also have properties relevant to fault-tolerant quantum computation [17]. Very recently [18–20], it was suggested that lattice-FQH states may similarly arise without a magnetic field, in fractionally filled topologically nontrivial bands.

In contrast to the IQH and QSH effects, which can be fully understood in terms of non-(or weakly-) interacting electrons, interactions are an essential requirement for FQH states, which places demanding restrictions on candidate systems: One needs a topologically nontrivial band that must be nearly flat—similar to the highly degenerate Landau levels—so that the electron-electron interaction can at the same time be large compared to the band width and small compared to the gap separating it from other bands [18–20]. If the requirements can be fulfilled, however, the temperature scale of the FQH state is set by the

energy scale of the interaction. This can allow temperatures considerably higher than the sub-Kelvin range of the conventional FQH effect, which would be extremely desirable in view of potential quantum-computing applications. Moreover, the lattice version of FQH states [21] may have unique and different properties. [22].

In most recently proposed model Hamiltonians [18–20,23–25], the topological nature of the bands was introduced by hand and model parameters have to be carefully tuned to obtain very flat bands. As potential realizations, ''purpose built'' physical systems in oxide heterostructures [26] or optical lattices [19] were suggested. On the other hand, topologically nontrivial bands can in principle emerge spontaneously in interacting electron systems [27,28]; e.g., for charge-ordered systems [29,30] or for electrons coupling to spins in a noncoplanar magnetic order [31,32]. We demonstrate here that such a scenario indeed arises in a Hubbard model describing electrons with a t_{2g} orbital degree of freedom on a triangular lattice: a ground state with topologically nontrivial and nearly flat bands is stabilized by onsite Coulomb interactions. Upon doping the flat bands, longer-range Coulomb repulsion induces FQH states.

t_{2g} orbitals on the triangular lattice.—The building blocks of our system are oxygen octahedra with a transition-metal (TM) ion in the center, the most common building block in the large and versatile material class of TM oxides. Local cubic symmetry due to the oxygen ions splits the d-orbitals into t_{2g} and e_g levels, and it has been shown that orbital degrees of freedom of either kind can substantially reduce the width of topologically nontrivial bands [24]. Here, we concentrate on the t_{2g} orbitals illustrated in Fig. 1(a), which are further split by a crystal field due to the overall lattice geometry. On a triangular lattice, we find one a_{1g} and two $e'_{g,\pm}$ states, see Fig. 1(b), with a splitting $H_{\rm JT} = \Delta_{\rm JT}(n_{e_{g+}} + n_{e_{g-}} - 2n_{a_{1g}})/3$ depending on the Jahn-Teller effect and the lattice [33]. Electron hopping
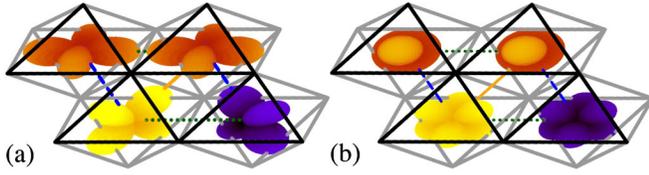
FIG. 1 (color online). Triangular perovskite lattice and t_{2g} orbitals. Oxygen octahedra are indicated by lines, with black lines illustrating the front facets. Thick dotted (dashed, solid) lines indicate nearest-neighbor bonds along lattice vector $\mathbf{a}_1$ ($\mathbf{a}_2$, $\mathbf{a}_3$). (a) Shows two d_{xy} orbitals (top) and one d_{xz} and d_{yz} orbital (bottom). In (b), the orbitals reflecting the threefold lattice symmetry are shown: The two e'_g orbitals (bottom), which differ by their complex phases, will turn out to be half filled, while the a_{1g} orbital (pointing out of the plane, see top) forms nearly flat bands with nontrivial topological character that can support spontaneous FQH states.

along nearest-neighbor (NN) bonds consists of terms t via ligand oxygens and t_{dd} due to direct d-d overlap [33,34], hopping matrices are given in [35]. We set here $n < 3$ and choose $t > 0$ [33] as unit of energy, but analogous results hold for $n > 3$, $t < 0$, and $t_{dd} \rightarrow -t_{dd}$, $\Delta_{JT} \rightarrow -\Delta_{JT}$ due to particle-hole symmetry.

In TM oxides, Coulomb interaction is substantial compared to the kinetic energy of t_{2g} orbitals and spin-orbital physics induced by correlations are known to be rich in t_{2g} systems on triangular lattices [34,36]. We take into account the onsite interaction including Coulomb repulsion U (intraorbital) and U' (interorbital) as well as Hund's-rule coupling J. We employ a mean-field approximation with a decoupling into expectation values of densities $\langle n_{\mathbf{i},\alpha,\sigma} \rangle = \langle c^\dagger_{\mathbf{i},\alpha,\sigma} c_{\mathbf{i},\alpha,\sigma} \rangle$ for site $\mathbf{i}$, orbital α, and spin σ [37,38]. The spin is thus reduced to its z component $m_{\mathbf{i},\alpha} = (n_{\mathbf{i},\alpha,\uparrow} - n_{\mathbf{i},\alpha,\downarrow})/2$ and noncollinear magnetic patterns are treated by allowing for a site-dependent spin-quantization axis expressed by angles θ_i and ϕ_i. The change in quantization axis from site to site manifests itself in a complex Berry phase for the hopping terms [39]. Numerical optimization is used to find the θ_i and ϕ_i giving the magnetic ground state, permitting arbitrary magnetic orderings with unit cells of up to four sites, including all phases considered in Ref. [40]. For simplicity, we present here results for $J/U = 1/4$ and the relation $U' = U - 2J$ between the Kanamori parameters was used, but we have verified that the results presented remain robust for other choices. For details see [35].

For wide parameter ranges (see below), the ground state is the noncoplanar spin-chiral phase illustrated in Figs. 2(a) and 2(b). As demonstrated in the context of the Kondo-lattice [38,40] and the Hubbard [38,41] models, this magnetic order leads to topologically nontrivial bands, which can also be seen in the one-particle bands shown in Fig. 2(c). The chemical potential lies within the a_{1g} states of the lower Hubbard band, where the electron spin is
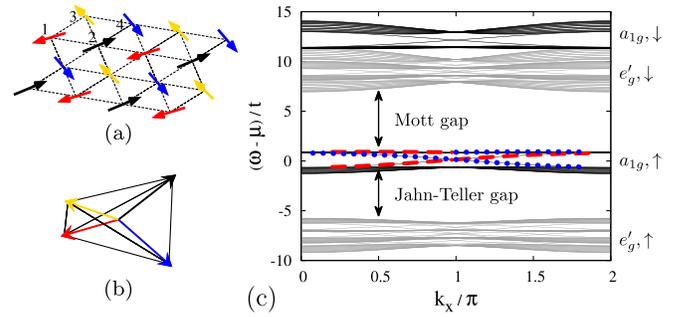

FIG. 2 (color online). Spin-chiral magnetic phase with topologically nontrivial bands stabilized by onsite Coulomb interactions in t_{2g} electrons on a triangular lattice. (a) Chiral magnetic order, the sites of the unit cell are labeled by 1 to 4. (b) The spins on the four sites can be seen as pointing to the corners of a tetrahedron; i.e., the pattern is noncoplanar. (c) One-particle energies on a cylinder (periodic boundary conditions along x) in the mean-field [35] ground state of the t_{2g} multiorbital Hubbard model, which is given by the pattern shown in (a). States drawn in black (gray) have more (less) than 33% a_{1g} character, dashed and dotted lines indicate edge states with more than 33% of their weight on the top (bottom) row of sites. The arrows $\uparrow$ ($\downarrow$) indicate states with electron spin mostly (anti-) parallel to the local quantization axis, which can be seen as the lower (upper) Hubbard band. The filling is 2.5 electrons per site, slightly less than half filling. Parameters used were $t = 1$, $t_{dd} = 0$, $U/t = 12$, $J/t = 3$, $\Delta_{JT}/t = -6$. The figure of merit M, which is given by the ratio of the gap separating the two a_{1g} subbands of the lower Hubbard band and the band width of the highest subband of the lower Hubbard band, is $M \approx 14$.

mostly parallel (labeled by $\uparrow$) to the direction defined by the spin-chiral pattern. Dashed and dotted lines decorate states living on the top and bottom edges of a cylinder, they cross the chiral gap exactly once as one left- and one right-moving edge mode, indicating the different Chern numbers associated with the two bands directly above and below the chemical potential. Such a spontaneous IQH state is already rather exotic and has recently been shown to support fractionalized excitations bound to vortices [42].

Figure 2(c) also indicates that the upper chiral subband has a very small width, ~ 14 times smaller than the chiral gap. One can quantify the band flatness by a figure of merit M given by the ratio of the gap to the band width. Its dependence on various parameters of the Hamiltonian is shown in Fig. 3. It peaks at $M > 40$, but the more striking observation is that it is above 5 or even 10 for wide ranges of U, Δ_{JT} and t_{dd}, in contrast to many other proposals that require carefully fine-tuned parameters [18–20,23–25,43]. Nearly flat chiral bands are thus very robust in this system and both their topological character and their flat dispersion emerge spontaneously with purely onsite interaction and short-range hopping, without spin-orbit coupling or any explicit breaking of time-reversal symmetry.

Mapping to an effective model.—For large onsite interactions and large crystal-field splitting $U, J, |\Delta_{JT}| \gg t, t_{dd}$,
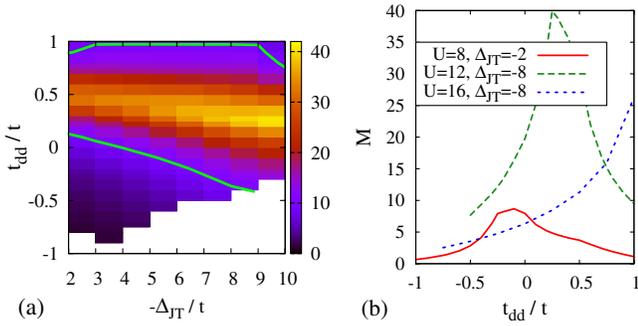
FIG. 3 (color online). Stability of the spin-chiral phase and flatness of the topological bands depending on parameters of the Hamiltonian. In (a), shaded areas in the t_{dd}-Δ_{JT} plane indicate a spin-chiral ground state Fig. 2(a) and 2(b) for $U/t = 12$, white areas have a different ground state. Shading indicates the figure of merit M for the flatness of the upper chiral subband, bright thick lines bound the region with $M \geq 10$. (b) shows M depending on t_{dd} for selected sets of U and Δ_{JT}. Where the "Mott gap", which separates the flat topologically nontrivial band from the upper Hubbard band, becomes very small, M is determined by the minimal gap separating the band of interest from other bands. $J = U/4$ and $t = 1$ were used in all cases.

the three-orbital model with fillings between 2 and 3 electrons per site can be mapped onto the one-band Kondo-lattice model (KLM). Low-energy configurations minimize onsite interactions and thus contain two or three electrons per site, with parallel spins due to Hund's rule. In order to additionally minimize the crystal-field energy, the e'_g levels will always be half filled and form an effective spin, while any holes will be found in the a_{1g} sector. The electrons in the partially filled a_{1g} states can delocalize with an isotropic hopping $t_{a1g} = (2t + t_{dd})/3$; however, their spin must remain parallel to the local e'_g spin. In the low-energy limit, each site can thus be described as a spin coupled to a charge degree of freedom and we arrive at the situation described by the KLM in the limit of strong Hund's rule coupling. Our numeric mean-field results corroborate this picture; see Fig. 2(c), where the e'_g levels are found far below the chemical potential. The KLM supports spin-chiral phases on many frustrated lattices like the triangular [38,40,44,45], pyrochlore [46], and face-centered cubic [47] lattices.

In addition to processes within the low-energy Hilbert space, virtual excitations involving high-energy states can be taken into account in second-order perturbation theory. This leads to (i) effective longer-range hopping of the a_{1g} electrons and (ii) an effective antiferromagnetic superexchange between the e'_g spins. The latter stabilizes the spin-chiral pattern [45] and is due to excitations into the upper Hubbard/Kondo band. When it is suppressed for $U \gtrsim 24|t|$, the ground state consequently becomes FM, as in the KLM with a large Kondo gap [40,44]. Nevertheless, the exotic spin-chiral state is remarkably stable in the present t_{2g} system considering its sensitivity to Hund's coupling in the KLM [40].

The effective longer-range hopping of a_{1g} electrons involves processes via excitations into the upper Kondo/Hubbard band ($\propto 1/J$ and $\propto 1/U$) as well as virtual excitations of e'_g electrons into a_{1g} states ($\propto 1/\Delta_{JT}$); for details see [35]. Second-neighbor hopping $\propto 1/J$ does not significantly modify the low-energy bands and drops out completely in the limit of a large Mott/Hubbard gap, but third-neighbor hopping t_3 is crucial in cancelling the dispersion coming from NN hopping t_1 for one of the bands [35]. The simplest description of the effective low-energy bands around the Fermi level is thus

$$H_{\text{eff}}(\mathbf{k}) = 2t_1 \sum_j \sigma^j \cos \mathbf{k} \mathbf{a}_j + 2t_3 \sum_j \sigma^0 \cos 2\mathbf{k} \mathbf{a}_j, \quad (1)$$

where $\mathbf{a}_j$ ($j = 1, 2, 3$) denote the unit vectors on the triangular lattice. Pauli matrices σ^j and unit matrix σ^0 refer to the two sites of the electronic unit cell in the chiral phase [38]. Formally, this describes electrons moving in a constant (and very strong) magnetic field with a flux of $\pi/2$ threading each triangle of the lattice [38].

FQH ground states of an effective spinless one-band model.—We now address the impact of NN Coulomb interaction $V \sum_{\langle i,j \rangle} n_i n_j$ on the fractionally filled flat band. The spin-chiral state can only be expected to remain stable for densities close to 2.5 electrons per site, i.e., low doping factions ν of the flat band [40]. FQH states corresponding to such low fillings are generally separated from the rest of the spectrum by only a small gap, making their analysis on finite-size clusters difficult [48]. Here, we use Lanczos exact diagonalization [20,35,43,48] to study a number of simple filling fractions (1/3, 2/3, 1/5, and 2/5) available on accessible lattices and consistently find V to induce signatures of a FQH state. It is thus plausible that the FQH behavior discussed next persists to fractional fillings in a low doping range of the spin-chiral state.

As an example, we present here the case of 16 electrons on a 4×6-site cluster of the model Eq. (1), a filling that would correspond to $2.\dot{6}$ in the original three-orbital model. After a particle-hole transformation, it corresponds to 2/3 filling of the nearly flat band. Figure 4(a) shows that with increasing V, three low-energy states split off from the rest of the spectrum. Inserting a magnetic flux $\phi_y = 2\pi$ interchanges the three states, $\phi_y = 6\pi$ recovers the original situation, see Fig. 4(b), as reported for other systems [20,24,43]. The Chern number C is evaluated by integrating the flux-dependent Berry curvature $\Omega^n(\phi_x, \phi_y)$ (obtained by the Kubo formula [35,49,50]) over the square $0 \leq \phi_x, \phi_y < 6\pi$. For $V = 0.2|t|$, the three low-energy states have Chern numbers within 1% of the expected $C = 2/3$, a deviation well within the limits of reported finite-size effects [20].

Conclusions.—The possibility of a spontaneous FQH effect without a magnetic field is currently hotly discussed, and various models have been suggested [18–20,23–26,43]. However, an experimental realization appears
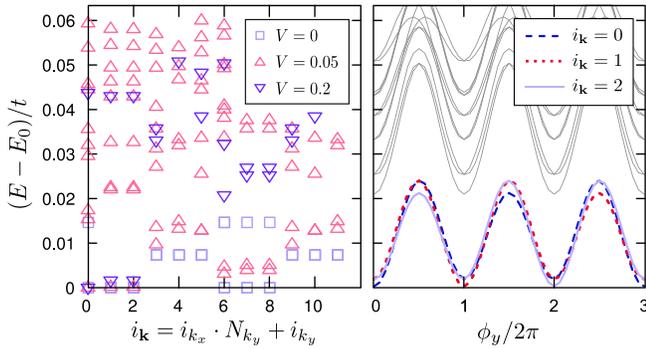
FIG. 4 (color online). FQH state induced by NN Coulomb repulsion V in the effective one-band model Eq. (1). (a) Energy depending on total momentum **k** for several values of V/t. (b) Energy for $V/t = 0.2$ depending on a flux ϕ_y added whenever an electron goes once around the whole lattice in y direction. Each addition of $\phi = 2\pi$ leads to an equivalent state, 6π to the same state. The Chern numbers associated with the three low-energy states are almost exactly $2/3$ for $V/t = 0.2$. Lattice size is 4×6 sites (12 two-site unit cells), parameters in Eq. (1) are $t_1 = 0.27t$ and $t_3 = -0.06t$, giving bands with $M \approx 13$ and a gap of $0.89t$. The filling of the flat band is $2/3$.

challenging, as the necessary topological character and the flatness of the bands need to be carefully engineered in previous proposals. We have shown here that bands with the desired properties emerge spontaneously for wide parameter ranges in strongly correlated t_{2g} orbitals on a triangular lattice, and that these bands support FQH ground states. Both t_{2g} systems and triangular lattices occur in various TM oxides, and signatures of the unconventional *integer* QH state have been reported for a triangular-lattice palladium-chromium oxide [51]. This harbors the prospect that a suitable material can be synthesized in this highly versatile material class. As such a material is by default strongly correlated, one also naturally expects an intersite Coulomb repulsion that is strong enough to stabilize spontaneous FQH states in the absence of a magnetic field.

[1] K. v. Klitzing, G. Dorda, and M. Pepper, Phys. Rev. Lett. **45**, 494 (1980).
[2] D. J. Thouless, M. Kohmoto, M. P. Nightingale, and M. den Nijs, Phys. Rev. Lett. **49**, 405 (1982).
[3] F. D. M. Haldane, Phys. Rev. Lett. **61**, 2015 (1988).
[4] C. L. Kane and E. J. Mele, Phys. Rev. Lett. **95**, 146802 (2005).
[5] L. Fu, C. L. Kane, and E. J. Mele, Phys. Rev. Lett. **98**, 106803 (2007).
[6] R. Roy, Phys. Rev. B **79**, 195322 (2009).
[7] J. E. Moore and L. Balents, Phys. Rev. B **75**, 121306 (2007).
[8] B. A. Bernevig and S.-C. Zhang, Phys. Rev. Lett. **96**, 106802 (2006).
[9] M. Hasan and C. Kane, Rev. Mod. Phys. **82**, 3045 (2010).
[10] X.-L. Qi and S.-C. Zhang, Rev. Mod. Phys. **83**, 1057 (2011).
[11] H. Zhang, C.-X. Liu, X.-L. Qi, X. Dai, Z. Fang, and S.-C. Zhang, Nature Phys. **5**, 438 (2009).
[12] Y. Xia, D. Qian, D. Hsieh, L. Wray, A. Pal, H. Lin, A. Bansil, D. Grauer, Y. S. Hor, R. J. Cava, and M. Z. Hasan, Nature Phys. **5**, 398 (2009).
[13] B. A. Bernevig, T. L. Hughes, and S.-C. Zhang, Science **314**, 1757 (2006).
[14] M. Konig, S. Wiedmann, C. Brune, A. Roth, H. Buhmann, L. W. Molenkamp, X.-L. Qi, and S.-C. Zhang, Science **318**, 766 (2007).
[15] D. C. Tsui, H. L. Stormer, and A. C. Gossard, Phys. Rev. Lett. **48**, 1559 (1982).
[16] R. B. Laughlin, Phys. Rev. Lett. **50**, 1395 (1983).
[17] C. Nayak, S. H. Simon, A. Stern, M. Freedman, and S. Das Sarma, Rev. Mod. Phys. **80**, 1083 (2008).
[18] E. Tang, J.-W. Mei, and X.-G. Wen, Phys. Rev. Lett. **106**, 236802 (2011).
[19] K. Sun, Z. Gu, H. Katsura, and S. D. Sarma, Phys. Rev. Lett. **106**, 236803 (2011).
[20] T. Neupert, L. Santos, C. Chamon, and C. Mudry, Phys. Rev. Lett. **106**, 236804 (2011).
[21] X.-L. Qi, Phys. Rev. Lett. **107**, 126803 (2011).
[22] M. Barkeshli and X.-L. Qi, arXiv:1112.3311.
[23] X. Hu, M. Kargarian, and G. A. Fiete, Phys. Rev. B **84**, 155116 (2011).
[24] J. W. Venderbos, M. Daghofer, and J. van den Brink, Phys. Rev. Lett. **107**, 116401 (2011).
[25] Y.-F. Wang, Z.-C. Gu, C.-D. Gong, and D. N. Sheng, Phys. Rev. Lett. **107**, 146803 (2011).
[26] D. Xiao, W. Zhu, Y. Ran, N. Nagaosa, and S. Okamoto, Nature Commun. **2**, 596 (2011).
[27] S. Raghu, X.-L. Qi, C. Honerkamp, and S.-C. Zhang, Phys. Rev. Lett. **100**, 156401 (2008).
[28] K. Sun, H. Yao, E. Fradkin, and S. A. Kivelson, Phys. Rev. Lett. **103**, 046811 (2009).
[29] G. A. Fiete, V. Chua, X. Hu, M. Kargarian, R. Lundgren, A. Ruegg, J. Wen, and V. Zyuzin, arXiv:1106.0013 [Physica E (Amsterdam) (to be published)].
[30] S. Nishimoto, M. Nakamura, A. O'Brien, and P. Fulde, Phys. Rev. Lett. **104**, 196401 (2010).
[31] P. Matl, N. Ong, Y. Yan, Y. Li, D. Studebaker, T. Baum, and G. Doubinina, Phys. Rev. B **57**, 10 248 (1998).
[32] Y. Taguchi, Y. Oohara, H. Yoshizawa, N. Nagaosa, and Y. Tokura, Science **291**, 2573 (2001).
[33] W. Koshibae and S. Maekawa, Phys. Rev. Lett. **91**, 257003 (2003).
[34] H. F. Pen, J. van den Brink, D. I. Khomskii, and G. A. Sawatzky, Phys. Rev. Lett. **78**, 1323 (1997).
[35] See Supplemental Material at http://link.aps.org/supplemental/10.1103/PhysRevLett.108.126405 for details on the parameters, numerical methods, and the mapping to the one-band model.
[36] B. Normand and A. M. Oleś, Phys. Rev. B **78**, 094427 (2008).
[37] T. Nomura and K. Yamada, J. Phys. Soc. Jpn. **69**, 1856 (2000).

[38] I. Martin and C. D. Batista, Phys. Rev. Lett. **101,** 156402 (2008).

[39] E. Dagotto, *Nanoscale Phase Separation and Colossal Magnetoresistance* (Springer, Berlin, 2002).

[40] Y. Akagi and Y. Motome, J. Phys. Soc. Jpn. **79,** 083711 (2010).

[41] T. Li, arXiv:1103.2420.

[42] R. A. Muniz, A. Rahmani, and I. Martin, arXiv:1112.3347.

[43] D. N. Sheng, Z.-C. Gu, K. Sun, and L. Sheng, Nature Commun. **2,** 389 (2011).

[44] Y. Kato, I. Martin, and C. D. Batista, Phys. Rev. Lett. **105,** 266405 (2010).

[45] S. Kumar and J. van den Brink, Phys. Rev. Lett. **105,** 216405 (2010).

[46] G.-W. Chern, Phys. Rev. Lett. **105,** 226403 (2010).

[47] R. Shindou and N. Nagaosa, Phys. Rev. Lett. **87,** 116801 (2001).

[48] N. Regnault and B. A. Bernevig, arXiv:1105.4867.

[49] Q. Niu, D. Thouless, and Y.-S. Wu, Phys. Rev. B **31,** 3372 (1985).

[50] D. Xiao, M.-C. Chang, and Q. Niu, Rev. Mod. Phys. **82,** 1959 (2010).

[51] H. Takatsu, S. Yonezawa, S. Fujimoto, and Y. Maeno, Phys. Rev. Lett. **105,** 137201 (2010).